Experimental investigation of a PVT system performance using nano ferrofluids

CrossMark

Matin Ghadiri [a,*], Mohammad Sardarabadi [b], Mohammad Pasandideh-fard [b], Ali Jabari Moghadam [a]

[a] Department of Mechanical Engineering, University of Shahrood, Shahrood, Iran
[b] Department of Mechanical Engineering, Ferdowsi University of Mashhad, Mashhad, Iran

ABSTRACT

In this paper, the effects of ferrofluids as a coolant on the overall efficiency of a PVT (photovoltaic thermal unit) system are experimentally investigated. The fluids considered in the experiment are distilled water and a ferrofluid (Fe_3O_4-water) with 1% and 3% concentrations by weight (wt%). The experiments were performed in indoor conditions under two constant solar radiations (1100 W/m^2 and 600 W/m^2) using a solar simulator. Due to the unique characteristic behavior of ferrofluids, their rheological and thermo-physical properties can be changed under an external magnetic field. The ferrofluids in this study were placed under constant and alternating magnetic fields in the cooling section in order to investigate the effect of both types of magnetic fields on the overall efficiency of a PVT system. The results show that by using a 3 wt% ferrofluid, the overall efficiency of the system improved by 45% and when an alternating magnetic field with 50 Hz frequency was applied, the overall efficiency increased to about 50% compared to that of the distilled water as coolant fluid. The overall exergy output of the system with and without ferrofluids, was also compared with that of the PV system with no collector. It was observed that by adding a thermal collector to a PV system and using a 3 wt% ferrofluid under an alternating magnetic field, the total exergy can be increased as high as 48 W.

© 2015 Elsevier Ltd. All rights reserved.

1. Introduction

The global need for energy savings requires the usage of renewable sources in many applications. One of the most important of these applications is a Photovoltaic (PV) cell which converts solar radiation into electricity. Based on the general diode equation that expresses the behavior of a simple photovoltaic system, increasing the cell temperature decreases the open circuit voltage which causes a drop of electricity conversion efficiency. But even under a standard test condition the efficiency of a PV system ranges from 4% to 17% [1]. More than 50% of the incident solar energy is absorbed and the rest of irradiation is reflected. The absorbed heat leads to serious problems such as the increase of the PV cell working temperature. For example, the efficiency of a typical PV system with c-Si cells is decreased by 0.45% for one degree Celsius increase of the working temperature [2]. The increased temperature can also cause a permanent structural damage of the module if the thermal stress remains for a prolonged period [1]. One remedy to avoid the temperature increase of the PV system is the use of a

photovoltaic-thermal hybrid solar system (or PVT) where the unfavorable absorbed heat from the cells is collected through an additional thermal unit. Therefore, a PVT system consists of photovoltaic and solar thermal components which produce both electricity and heat from one integrated component. PVT systems have been studied considerably in the literature by all means of analytical solutions, experimental measurements, and numerical simulations. Numerous studies focused on cooling methods of solar cells using water and air as the heat removal media [3–6].

Chow et al. [7] numerically and experimentally investigated energy and exergy analysis of a PVT water based collector system with and without a glass cover. They evaluated the effects of six operating parameters on the system efficiency from the viewpoint of the first and second laws of thermodynamics. The parameters included the cell efficiency, packing factor, mass flow rate, wind velocity, radiation and ambient temperature. Gang et al. [8] presented a numerical and experimental study on a heat pipe PVT system. The numerical results for the temperature compared well with those of the experiments with less than 5% discrepancy. They measured the electrical and thermal average efficiencies to be 9.4% and 41.9%, respectively. Dubey et al. [9] introduced an analytical method to obtain the electrical efficiency of a PVT hybrid air collector with and without a duct. They found that the annual

---

Nomenclature

A	area (m^2)	ρ	density (kg/m^3)
Cp	specific heat (J/kg °C)	ϕ	nanoparticles volume fraction
$\dot{E}$	energy rate (W)	v	arbitrary parameter
$\dot{Ex}$	exergy rate (W)		
FF	filled factor		*Subscripts*
G	incident radiation (W/m^2)	a	ambient
I	electrical current (A)	c	collector
m	mass (kg)	el	electrical
$\dot{m}$	mass flow rate (kg/s)	f	fluid
P	electrical power (W)	f, i	fluid inlet
PVT	photovoltaic thermal unit	in	input
$\dot{Q}$	heat transfer rate (W)	m	maximum
R	arbitrary function	n	nanoparticle
r	packing factor	nf	nanofluid
T	temperature (°C)	oc	open circuit
V	voltage (V)	f, o	fluid outlet
		pv	photovoltaic
Greeks		pvt	photovoltaic thermal
δ	uncertainty	sc	short circuit
η	energetic efficiency	th	thermal

---

average electrical efficiency of a PV module with forced air circulation is about 0.66% larger than a PV module without cooling. Bahaidarah et al. [10] presented a numerical and experimental study to evaluate the performance of a PV module by a surface water cooling system installed on the back of the module for hot climatic conditions. They observed that adding an active cooling technique dropped the operating temperature of the module by about 20%, and increased the electrical efficiency by nearly 9%. Daghigh et al. [11] reviewed the various types of liquid base PVT collectors in the past few decades.

Generally, fluids have lower thermal conductivity in comparison with metal suspensions. Therefore, dispersion of nano-sized particles of different materials (metals, metal oxides, etc.) in a carrier fluid known as nanofluids has been the subject of intensive investigations over the recent decades due to their potential applications in heat transfer and electronic coolings. Yun and Qunzhi [12] used a film of MgO/water nanofluid with different concentrations of 0.02%, 0.06% and 0.1% by weight, on top of silicon photovoltaic cells in order to absorb the extra heat from the cells. They investigated the effects of the nanofluid film thickness on the output power of solar cells. They found that an increase of the film thickness or the concentration of the nanofluid, reduces the thermal and electrical efficiencies at a constant solar radiation. Yousefi et al. [13] performed experiments to study the effects of using Al$_2$O$_3$/water nanofluid as a heat absorber medium in a flat plate solar water heater collector. They considered the effects of mass flow rate and nanoparticles mass fraction on the efficiency of the collector. They examined various mass flow rates of 1, 2, and 3 L/min and two different nanofluid concentrations of 0.2% and 0.4% by weight (wt%). Their results showed that at a constant nanofluid concentration, increasing the mass flow rate increased the efficiency of the collector. Sardarabadi et al. [14] studied experimentally the effects of using silica-water nanofluid as a coolant on the thermal and electrical efficiencies of a PVT system. The silica-water nanofluid used in this study were 1% and 3% by weight (wt%). They found that the thermal efficiency of the PVT collector for the two cases of 1 wt% and 3 wt% of nanofluids are increased by 7.6% and 12.8%, respectively.

Magnetic nanofluids (or nano ferrofluids) are one kind of nanofluids consisting of *superparamagnetic* nanoparticles suspended in a nonmagnetic carrier fluid. These fluids are modern set of nanofluids due to their unique characteristics behavior as smart or functional fluids. Their properties such as viscosity and conductivity can be changed under an external magnetic field and their rheological characteristics can be accurately controlled. These properties and especially their capability of heat transfer enhancement make this kind of fluid an interesting issue for many researchers. Due to its unique characteristics, the ferrofluids have been progressively employed in various applications in many engineering fields such as electronic, mechanical, aerospace and bioengineering. Li et al. [15] measured the convective heat transfer coefficient of the aqueous magnetic fluid flow around a heated wire in both a uniform magnetic field and a magnetic field gradient; they analyzed the effects of the external magnetic field strength and orientation on the thermal behavior of the ferrofluid. They found that controlling the heat transfer process of a ferrofluid flow is affected by both the orientation and magnitude of an external magnetic field. Lajvardi et al. [16] investigated experimentally the convective heat transfer of a ferrofluid flowing through a heated copper tube in the laminar regime in the presence of a magnetic field. They investigated the strength of the magnetic field, the effect of magnetic nanoparticles concentrations, and the magnet position on the heat transfer of ferrofluid. Ghofrani and Dibaei [17] presented an experimental investigation on forced convection heat transfer of an aqueous ferrofluid in the presence of an alternating magnetic field under a uniform heat flux and laminar flow conditions. They measured and compared the convective heat transfer coefficient for distilled water and ferrofluid under various conditions and investigated the effects of alternating magnetic field, volume concentration and the Reynolds number. Their results showed a maximum of 27.6% enhancement in the convection heat transfer. Azizian et al. [18] investigated the effect of an external magnetic field on the convective heat transfer and pressure drop of a ferrofluid under laminar flow regime conditions (Re < 830). They reported that the effect of the magnetic field on the pressure drop is not as significant. The pressure drop increased only by up to 7.5% when a magnetic field intensity of 430 mT (milli Tesla) was applied; however, the local heat transfer coefficient of the ferrofluid was increased significantly (up to 300%). It was observed that the heat transfer enhancement is a function of flow rate (the Re number) and the magnetic field strength and gradient.
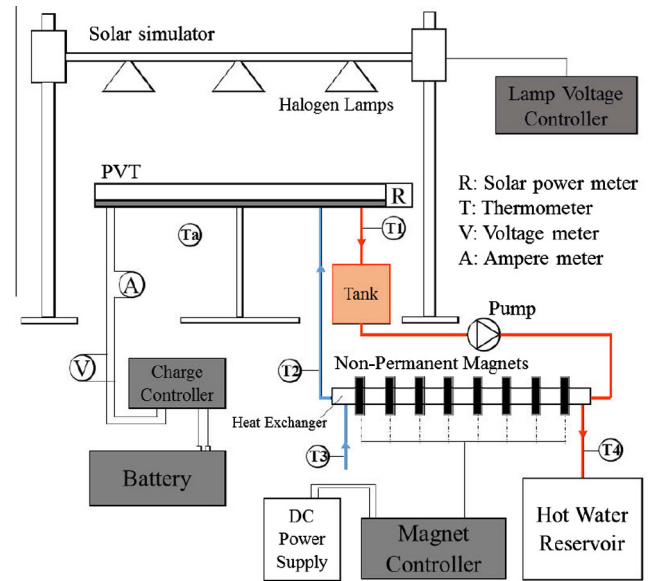
Fig. 1. A view of the experimental setup.

Fig. 2. A schematic diagram of the experimental setup.

Fig. 3. Structure of the PVT system.

Research studies on ferrofluids in solar applications are rare in the literature. In this paper, therefore, an experimental study is performed to investigate the effects of a ferrofluid on the efficiency of a PVT system under a constant and alternating magnetic field. The ferrofluid considered was Fe_3O_4-water nanofluid. Both thermal (in terms of energy and exergy) and electrical efficiencies of a PVT system with a flat plate collector were studied. Extensive experiments were performed in an indoor simulation to measure various parameters for the cases considered.

2. Experimental setup

2.1. Apparatus

An experimental setup was built to investigate the effect of the ferrofluid on the efficiency of a PVT (photovoltaic thermal units) system with a magnetic field. The photograph and a schematic diagram of the experimental setup are shown in Figs. 1 and 2, respectively. The experimental PVT setup consists of two 40 W mono-crystalline silicon photovoltaic modules (Suntech Co., China) and each of these PV modules consists of 36 solar cells. One of the photovoltaic units is equipped with a collector while the other one has no collector. Both units are tested in exactly the same conditions. Because of a simple design with only 2% lower efficiency compared to other types of collectors [19], a sheet and tube collector is utilized in this study. The solar cells are attached to the top surface of a thin copper plate soldered on the back to a serpentine copper tubing with a thermal insulation layer beneath (Fig. 3 and Table 1). To have a closed flow circuit (for the working fluid), a shell-and-tube heat exchanger with a counter flow design is used to cool the working fluid after being heated in the PVT collector. The mass flow rate of the working fluid is adjusted to 30 L/h. The second fluid used in this heat exchanger is the running city water with 40 L/h mass flow rate. There were 4 K-type thermocouples to measure flow temperatures at the inlet and outlet of the heat exchanger; they were installed inside the tube to measure the flow temperature more accurately. A 4-channels data logger (Testo-175) was used to acquire the temperature values. The heat exchanger, the thermocouples and all other connections were well insulated to minimize the heat loss. The working fluid was stored in a tan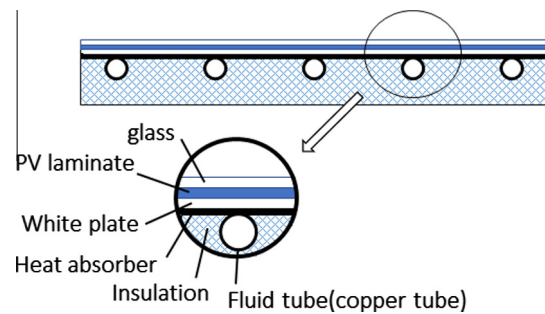k connected to a pump in order to circulate the fluid around the panel. Because of a low pressure of the system considered in this study, the connections between the parts were established with pneumatic connectors and fittings.

2.2. Solar simulator

The experiments were performed in an indoor condition due to its flexibility with respect to time and location. Therefore, a solar simulator is employed to imitate the necessary solar irradiation in the testing of photovoltaic modules section. The solar simulator has 9 tungsten halogen lamps each having 500 W arranged in 3 × 3 matrices to produce uniform distribution of irradiance. The position of each lamp can be adjusted in 3 directions. The tungsten-halogen lamps produce a continuous spectrum of light from near ultraviolet to the visible into the infrared. The color temperature is the temperature of an ideal black body radiator with the peak irradiance at the same wavelength as the test source. The tungsten halogen lamps as well as other filament lamps, can only work under maximum color temperature of 3500 K. They radiate weaker in the shorter wavelengths but stronger in the infrared regions compared to the color temperature of the sun which is approximately 5900 K. However, as filament temperature increases in a tungsten-halogen lamp and approaches the limiting melting point of tungsten, the proportion of visible wavelengths emitted by the lamp increases substantially. Due to the higher density of infrared emitted by the tungsten halogen lamps in

Table 1
Fabricated design parameters of PVT collector.

Type of PV cell:	Mono-crystalline silicon PV modules
Absorber plate and tube Materials:	copper
Absorber dimension	Plate: 630 mm × 540 mm
	Tube: ⌀ 10 mm
Method of joining	Gas welding + silicon adhesive

comparison to real sunlight, the readings indoor would be higher in thermal and lower in electrical.

This simulator can change the intensity between 100 W/m^2 and 2000 W/m^2 by decreasing/increasing the gap between lamps and photovoltaic modules. Also to have a uniform radiation all over the test section, a voltage controller was used to adjust the intensity of each lamp. The total incident radiation is measured by a solar power meter (TES/1333, Taiwan) mounted parallel to the photovoltaic surfaces. The maximum difference in the measured radiation at any point on the PV collector with the adjusted radiation was less than 6%.

2.3. Electrical Instrumentation

A circuit with a programmable microcontroller especially designed to control the supplying current of the magnet cores was employed in the experiments. This circuit had the ability to change the frequency and duty cycle (connection or disconnection time of the magnetic field) of alternating magnetic fields as well as to adjust the strength of both constant and alternating magnetic fields. The circuit had also the ability to manage how the magnets are turned on or off. An important feature of the circuit was in generating pulse waves with specific frequency and duty cycle for an alternating magnetic field. Eight non-permanent magnets made with zinc ferrite powder in the shape of U were used in the experiment. Eight magnets were placed in equal incremental distance along the heat exchanger placed inside the empty space of the magnets. With 2000 rounds of copper wire No. 20 wrapped around, these U cores were able to apply 300 G in the inside fluid flowing through the tube. The magnetic field magnitude was measured with an accurate Tesla meter. The other electrical structure of the system includes charge controllers, storage batteries, and DC load consumers (here two 20 W lamps). Charge controllers act as a connecting switch between batteries, load consumers and PV panels to assure a continuous electricity production in PV systems. Digital multimeters (VC9805, China) were used to measure short-circuit currents, and open-circuit voltages.

2.4. Ferrofluid characterisation and properties

Magnetic nano-particles of metal oxide such as Fe_3O_4, γ-Fe_2O_3 and spinel-type ferrites of MFe_2O_4 (with M = Mn, Co, Zn, Ni, etc.) are mostly used in ferrofluids due to their chemical stability [20]. These particles are produced using various methods such as, chemical co-precipitation, micro-emulsion and phase transfer [20,21]. In this study magnetite nanoparticles were generated from the chemical precipitation method [22] with a procedure explained as follows. First and before adding any salt, 200 ml of DI-water was bubbled with nitrogen gas (N_2) for 15 min continuously to prevent the solution from the reactions with oxygen (O_2). Then 5.12 g ferric chloride hexahydrate ($FeCl_3 \cdot H_2O$) and 2.00 g of ferrous sulfate ($FeSO_4$) were added to the water. Subsequently, the solution was stirred (with a 600 rpm) and heated slowly until reached a temperature of 80 °C. Next, under nitrogen atmosphere and stirring, ammonium hydroxide (NH_4OH with 1.5 M) was added drop-wise until pH exceeded 8 after which the solution turned black indicating the precipitation of iron oxide nanoparticles. The

temperature, stirring rate, and nitrogen bubbling conditions were maintained for 2 h. Finally, the generated black Fe_3O_4 nanoparticles were collected by an external magnet and separated from unwanted solution of NH_4OH. The nanoparticles were then washed with water several times to reach a neutral pH and dried in the air atmosphere [23]. The proper amount of resulted solid Fe_3O_4 powder was weighed by an electronic scale accurate to 0.001 g and dispersed in distilled water with a desired volume concentration. To stabilize the nanofluid, acetic acid ($C_2H_4O_2$) with a proper volumetric ratio was added to the solution before placing the ferrofluid under ultrasonic mixing. A sonication time of 30 min was found to produce a stable nanofluid for at least a month and with a mean diameter of 45 nm (Fig. 4)

The thermophysical properties of the prepared nanofluids are calculated from water and nanoparticles characteristics at the bulk temperature using following equations [24]:

$$\rho_{nf} = \phi \cdot \rho_n + (1 - \phi) \cdot \rho_f \tag{1}$$

$$C_{p,nf} = \frac{\phi \cdot (\rho_n \cdot C_{p,n}) + (1 - \phi)(\rho_f C_{pf})}{\rho_{nf}} \tag{2}$$

where ρ is the density and subscripts n, f and nf represent, nanoparticles, fluid, and nanofluid, respectively. ϕ is the volumetric ratio of nanoparticles in a suspension solution of the base fluid that can be calculated as:

$$\phi = \frac{m_n/\rho_n}{m_n/\rho_n + m_f/\rho_f} \tag{3}$$

where m_n and m_f are the mass of the nanoparticles and fluid, respectively.

3. Thermodynamic analysis

The overall performance of a mechanical system can be evaluated from different viewpoints such as thermodynamics, economics, and environmental implications. In this study, a thermodynamic approach based on the first and second laws similar to the works of Chow et al. [25] and Agrawal and Tiwari [26] is employed. The first and second laws of thermodynamics are also referred to energy and exergy analyses, respectively. While an energetic analysis determines the quantity of the energy, an exergetic analysis determines its quality.

3.1. Thermal and electrical efficiency

By considering the PV module and the thermal collector as a unified control volume, the input energy is the amount of solar radiation and the useful output energies are electrical and thermal energies. Therefore, the overall efficiency of a PVT system, η_{pvt} is equal to the ratio of the output energies to the input energy during
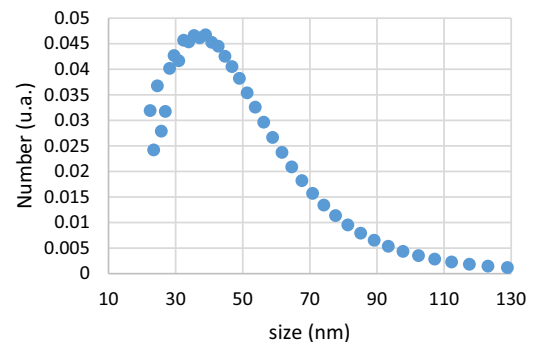
Fig. 4. Size dispersion by number of the synthesized Fe_3O_4 nano particles.

Table 2
Equipment and their accuracy.

Equipment and model	Measurement section	Accuracy
Solar power meter	Incident solar radiation	± 10 W/m^2 + 0.38
K type thermocouple	Fluid temperature	$\pm 0.15\,°C$ to $\pm 0.25\,°C$
Hg thermometer	Ambient temperature	$\pm 0.5\,°C$
Calibrated tube	Mass flow rate	± 1 ml
Stop watch	Mass flow rate	0.01 S
Digital multimeter	Voltage and Ampere	$\pm (0.5 + 1)$ V
		$\pm (0.5 + 1)$ A

a selected time period. Thus, the overall efficiency is the sum of the thermal and electrical efficiencies, η_{th} and η_{el}, respectively [7,27]:

$$\eta_{pvt} = \frac{\text{Total thermal energy} + \text{Total electrical energy}}{\text{Total solar irradiation over the collector}} \quad (4)$$

$$\eta_{pvt} \cong \frac{\dot{E}_{th} + \dot{E}_{el}}{\dot{E}_{in}} \Rightarrow \eta_{pvt} = \frac{\int_{t_1}^{t_2}(A_c\dot{E}_{th} + A_{pv}\dot{E}_{el})dt}{A_c \int_{t_1}^{t_2}(G)dt} = \eta_{th} + r \cdot \eta_{el} \quad (5)$$

where A_c and A_{pv} are the area of the collector and PV cells, respectively, and r is the packing factor defined as $A_c/A_{pv} \cdot \dot{E}_{th}$ is the rate of output thermal energy per unit area of the collector, $\dot{E}_{el}$ the rate of output electrical energy per unit area of photovoltaic cells and G the rate of the effective incident radiation per unit area of the collector. In Eq. (5), $\dot{E}_{th}$ can be calculated by a simple energy analysis as:

$$\dot{E}_{th} = \dot{m}_f \cdot C_{p,f} \cdot (T_{f,o} - T_{f,i}) \quad (6)$$

where $\dot{m}_f$ is the fluid mass flow rate through the collector, $C_{p,f}$ is the fluid specific heat, and $T_{f,i}$ and $T_{f,o}$ represent the fluid inlet and outlet temperatures, respectively. In Eq. (5), the electrical efficiency can be expressed as:

$$\eta_{el} = \frac{\dot{E}_{el}}{\dot{E}_{in}} = \frac{V_{oc} \times I_{sc} \times FF}{A_c G} \quad (7)$$

where V_{oc} is the open circuit voltage and I_{sc} is the short circuit current. FF (filled factor) is defined as the maximum power conversion efficiency of the PV that can be evaluated based on the ratio of the maximum power gained from the photovoltaic module to the open circuit voltage multiplied by the short circuit current at the standard test condition of the PV module [28]:

$$FF = \frac{P_m}{V_{oc} \times I_{sc}} \quad (8)$$

P_m is the maximum output electrical power (i.e., the ideal output power) given as:

$$P_m = V_m \times I_m \quad (9)$$

In order to analyze the PVT system based on the thermal energy, the output electrical energy must be converted into thermal energy because of the fact that from a thermodynamic point of view, one kWh of electricity cannot be directly compared with one kWh of heat. This is because the two types of energies do not have the same valuable quality; a conversion factor c_f (the conversion efficiency of thermal power plant which depends upon quality of coal) is, therefore, introduced in the literature [13,29,30,33] as:

$$\dot{E}_{el,th} = \frac{\dot{E}_{el}}{c_f} \quad (10)$$

For the most PVT fluid systems, a value of c_f between 0.35 and 0.40 has been introduced [29]; in this study, a medium value of 0.38 was used. Thus, the overall equivalent PVT efficiency (Eq. (5)) can be modified as:

$$\eta_{pvt} = \eta_{th} + r\left(\frac{\eta_{el}}{0.38}\right) \quad (11)$$

3.2. Overall thermal and exergy output

Similar to the overall efficiency of the system, the expression for the overall thermal output is defined as:

$$\dot{Q}_{overall} = \dot{Q}_{th} + \frac{\dot{Q}_{el}}{c_f} \quad (12)$$

The method by which the overall exergy output of the system can be calculated is similar to that of the energy output. By considering the photovoltaic module and the thermal collector as a unified control volume, the overall exergy output of the PVT system can be calculated as:

$$\dot{Ex}_{overall} = \dot{Ex}_{th} + \dot{Ex}_{el} \quad (13)$$

where

$$\dot{Ex}_{el} = \dot{E}_{el} \quad (14)$$

and

$$\dot{Ex}_{th} = \dot{E}_{th}\left(1 - \frac{T_a}{T_{f,o}}\right) \quad (15)$$

4. Uncertainty analysis

Evaluation of errors in the experiments is necessary to perform a valid test. In this study, the following equation is used for this purpose:

$$\delta R = \sqrt{\left(\frac{\partial R}{\partial v_1}\delta v_1\right)^2 + \left(\frac{\partial R}{\partial v_2}\delta v_2\right)^2 + \ldots + \left(\frac{\partial R}{\partial v_n}\delta v_n\right)^2} \quad (16)$$

where δR is the uncertainty of function R, δv_i the uncertainty of parameter v_i, and $\partial R/\partial v_i$ is the partial derivative of R with respect to parameter v_i. If the uncertainty in $v_1, v_2, \ldots, v_m, v_{m+1}, \ldots, v_n$ are independent, then the fractional uncertainty of R is written as [32]:

$$\frac{\delta R}{R} = \sqrt{\left(\frac{\delta v_1}{v_1}\right)^2 + \left(\frac{\delta v_2}{v_2}\right)^2 + \ldots + \left(\frac{\delta v_m}{v_m}\right)^2 + \left(-\frac{\delta v_{m+1}}{v_{m+1}}\right)^2 + \ldots + \left(-\frac{\delta v_n}{v_n}\right)^2} \quad (17)$$

The uncertainties associated with the measuring instruments of the experimental setup are reported in Table 2. Thus, the fractional uncertainties can be calculated for the thermal and electrical efficiencies and overall thermal and exergy output. The results are presented in Table 5. As Table 5 shows, the maximum absolute uncertainty for all parameters are less than 5% which is an indication of the reliability of the measured data in the experiment.

5. Results and discussion

In this study two sets of experiments are performed: one on a photovoltaic unit with a thermal collector (PVT system) and the other without (PV system). Two working fluids were employed: distilled water and a ferrofluid (Fe_3O_4-water) with two different volume concentrations (1 wt%, 3 wt%). The ferrofluid was tested in two conditions: one without a magnetic field and the other in presence of two kinds of constant and alternating magnetic field. For calculating the conversion efficiency of the system, the amount of consumed energy for pumping the coolant and generating the magnetic field has been calculated and subtracted from the total energy gained by the system; the consumed energy for the above purposes was not considerable.

5.1. Thermal and electrical efficiency variations of the system

The results presented in this study are given for five different cases: the collector with distilled water (Case 1), ferrofluid with
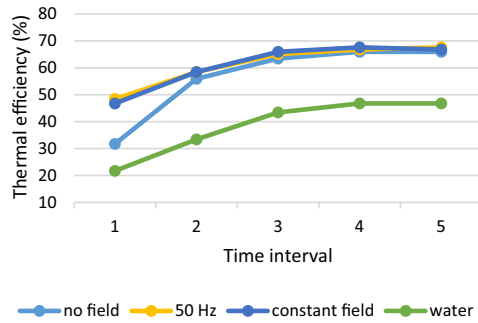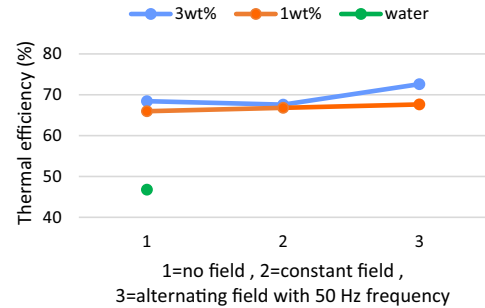
Fig. 5. Thermal efficiency for 1 wt% ferrofluid and distilled water under magnetic field (300G) for a solar radiation of 1100 W/m^2 and 30 L/h nano ferrofluid mass flow rate.

Fig. 7. Thermal efficiency for 1 wt% and 3 wt% ferrofluid and distilled water under magnetic field (300G) and 1100 W/m^2 radiation and 30 L/h nano ferrofluid mass flow rate.
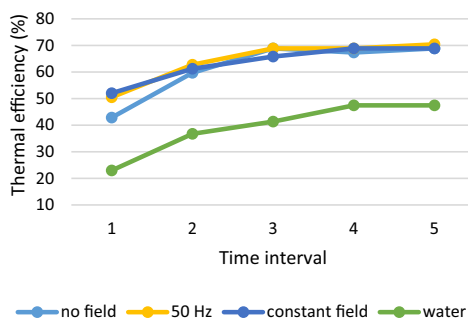
Fig. 6. Thermal efficiency for 1 wt% ferrofluid and distilled water under magnetic field (300G) for a solar radiation of 600 W/m^2 and 30 L/h nano ferrofluid mass flow rate.

no magnetic field (Case 2), ferrofluid with a constant magnetic field of 300G (Case 3), ferrofluid with an alternating magnetic field of 50 Hz with the same strength (Case 4), and finally, the PV system with no collector; i.e., the reference system (Case 5). The thermal efficiency variation of the PVT system under various conditions for a solar radiation of 1100 W/m^2 is shown in Fig. 5. The performance of the PVT system is recorded in each 15 min till the system reaches a steady-state condition (after nearly 1 h) where the system has the maximum overall efficiency. This has been the case for all experimental data presented in this paper. For the case of distilled water, when the system reaches the steady state condition, the thermal efficiency reaches a maximum of 46.77%. This value can be compared to that of the measurements performed by Fudholi et al. [31] where the thermal efficiency was reported to be around 50% for 800 W/m^2 radiation and 0.011–0.041 kg/s water mass flow rate. It should also be mentioned that the reported range of the thermal efficiency of a PVT system is between 25% and 75% depending on the experimental conditions, the amount of radiation, and the type of cooling system [8]. As seen from the figure, adding ferro nano-particles to water by 1 wt% under no magnetic field, increases the thermal efficiency to about 65.96%. Therefore, using ferrofluid instead of distilled water has a considerable effect on thermal efficiency of the system (an increase of 41%). The figure also reveals that applying a magnetic field, whether constant or alternating, has no significant effect on the system performance with ferrofluid as the working fluid. Fig. 6 shows the thermal efficiency variation of the PVT system for Case 1 to Case 4 under 600 W/m^2 solar radiation and 1 wt% magnetic nano particles. It is observed that the thermal efficiency for ferrofluid without any kind of magnetic field increases to 68.88%, whereas, this amount for distilled water is about 47.47%. Therefore, the thermal efficiency for the ferrofluid is increased by nearly 45%

compared to that of the distilled water. Once again, it is observed that the magnetic field does not affect the system performance.

As experimental observations show, the thermal efficiency of the system for 1 wt% magnetic nano particles for both radiations reached more than 40% compared to the case when the working fluid was distilled water. Particle migration, nanoparticle clustering, viscosity gradient and Brownian motion are several mechanisms identified as the probable reasons for heat transfer enhancement in nanofluids [15–17,20]. The increase of the thermal conductivity of the nanofluid along with the disturbed thermal boundary layer due to the addition of nano particles are among other reasons for the thermal efficiency increase.

In Fig. 7, the thermal efficiency of 3 wt% ferrofluid in comparison with 1 wt% ferrofluid and distilled water for Case 1 to Case 4 under a solar radiation of 1100 W/m^2 is shown. For Case 2 (ferrofluid with no magnetic field), the thermal efficiency for 3 wt% ferrofluid is enhanced to 68.42% which means that by tripling the ferrofluid concentration, about 4% improvement in the thermal efficiency is observed. The thermal efficiency for Case 3 and Case 4 for 3 wt% ferrofluid are 67.59% and 72.59%, respectively. Therefore, it can be concluded that using an alternating magnetic field with a frequency of 50 Hz (Case 4) increases the thermal efficiency of system by 6% in comparison to the case with no magnetic field (Case 2). It is also observed that the thermal efficiency for a constant magnetic field is very close to that of the system when no field is applied. As a result, using a constant magnetic field for a ferrofluid has almost no effect on the system performance.
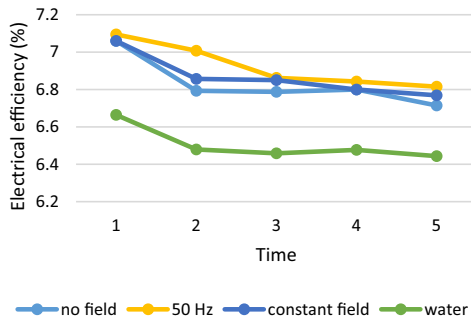
The thermal efficiency for the 3 wt% ferrofluid for the same cases as of Fig. 7 but under a solar radiation of 600 W/m^2 is presented in Fig. 8. As seen from the figure, the thermal efficiency of the system for Case 4 is about 74.96%, whereas, this amount for Case 2 and Case 3 is almost 71%. Similar to 1100 W/m^2 solar radiation, applying an alternating magnetic field improves the system
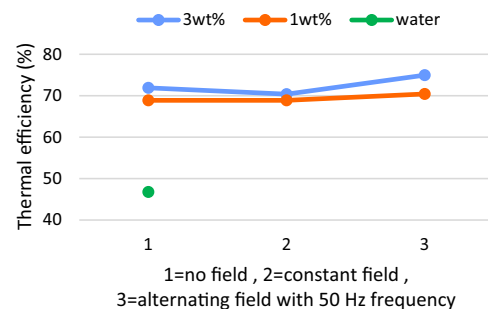

Fig. 8. Thermal efficiency for 1 wt% and 3 wt% ferrofluid and distilled water under magnetic field (300G) and 600 W/m^2 radiation and 30 L/h nano ferrofluid mass flow rate.
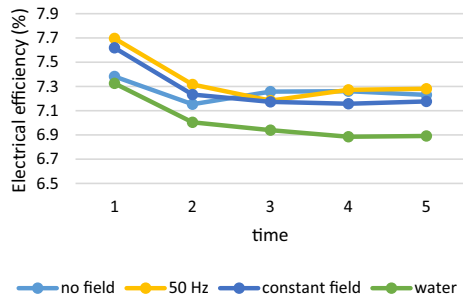
Fig. 9. Electrical efficiency for 3 wt% ferrofluid and distilled water under 1100 W/m² radiation and 30 L/h nano ferrofluid mass flow rate.
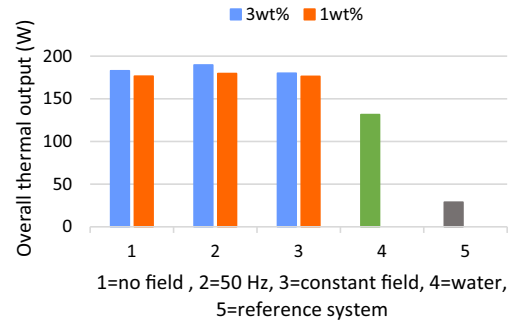

Fig. 10. Electrical efficiency for 3 wt% ferrofluid and distilled water under 600 W/m² radiation and 30 L/h nano ferrofluid mass flow rate.
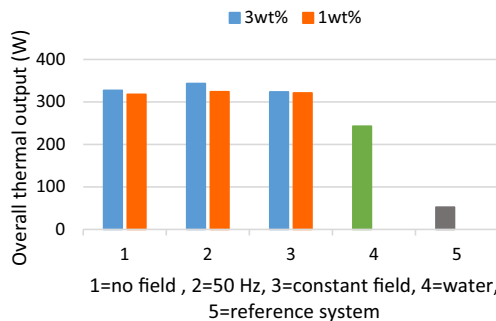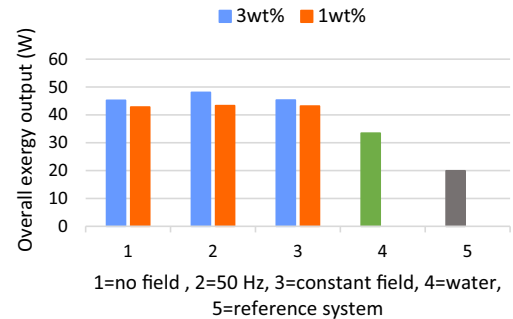

Fig. 11. Overall thermal output for 1 wt% and 3 wt% ferrofluid under magnetic field (300G) and 1100 W/m² radiation.

Fig. 12. Overall thermal output for 1 wt% and 3 wt% ferrofluid under magnetic field (300G) and 600 W/m² radiation.

Fig. 13. Overall exergy output for 1 wt% and 3 wt% ferrofluid under magnetic field (300G) and 1100 W/m² radiation.

performance slightly. The constant magnetic field, however, has no effect on the system.

From Figs. 7 and 8 it is clearly seen that by increasing the ferrofluid concentration from 1 wt% to 3 wt% the thermal efficiency of system is improved by 4%. Although this finding was expected as reported in the literature [20], the difference between the results for the two kinds of applied magnetic field is worth mentioning. The constant magnetic field is seen to have no considerable effect on the thermal efficiency. With applying alternating magnetic field, however, the thermal efficiency of system is increased. This phenomenon may be explained by ferro particle distribution and their cluster morphology. The presence of these particle clusters and their chained alignment due to the external magnetic field translates into more heat transfer in this case. Further details regarding the physical justification of heat transfer enhancement in presence of a field is available in the literature [16–18].

In Fig. 9, the electrical efficiency of 3 wt% ferrofluid and 1100 W/m² solar radiation for the cases (Case 1 to Case 4) is displayed. As the figure shows, for the PVT system the electrical efficiency reaches a value of 6.89% for Case 1, and 7.23% for Case 2 indicating that the electrical efficiency by using the ferrofluid is increased by nearly 4.8% compared to Case 1 with distilled water.

Fig. 10 shows the electrical efficiency of 3 wt% ferrofluid for the same cases and conditions as of Fig. 9 except for the solar radiation which is 600 W/m² in Fig. 10. It is also seen that for Case 2, the electrical efficiency is 6.71%, whereas, for Case 1 this amount is about 6.44% which again indicates an improvement in the system by using ferrofluid instead of distilled water as the working fluid.

Figs. 9 and 10 also reveal that the electrical efficiency is not significantly changed when a magnetic field is used for the ferrofluid under consideration. This result was expected because the magnetic field mainly affects the heat transfer in the cooling section of the system.

5.2. Overall thermal and exergy output of the system

The overall thermal and exergy output are calculated with the help of Eqs. (11), (12) for the entire cases at both of the solar radiations of 600 and 1100 W/m². Fig. 11 shows the variations of overall thermal output for 1100 W/m² solar radiation. As shown in the figure, the overall thermal output is 52.44 W for the reference system (Case 5), 242.90 W for the distilled water (Case 1), and 317.88 W and 327.25 W for Case 2 (ferrofluid with no magnetic field) for 1 wt% and 3 wt% ferrofluid concentrations, respectively. It is concluded that using ferrofluid instead of distilled water significantly enhances the overall thermal output of the system. The enhancement for 3 wt% ferrofluid is about 35% when compared to that of the distilled water. The overall thermal outputs for Case 3 for 1 wt% and 3 wt% are almost close to that of Case 2 which

Table 3
1 wt% Fe_3O_4 and distilled water.

	Radiation (W/m²)	$\Delta T_{collector}$ (°C)	η_{th} (%)	η_{el} (%)	η_{pvt} (%)	Overall thermal output (W)	Overall exergy output (W)
No field	1100	7.9	65.96	7.21	71.91	317.88	42.81
	600	4.5	68.88	6.68	74.40	176.52	18.78
5 Hz	1100	8.0	66.80	7.21	72.75	320.96	43.14
	600	4.5	68.88	6.64	74.36	176.29	18.43
25 Hz	1100	8.0	66.80	7.20	72.75	320.88	43.25
	600	4.5	68.88	6.69	74.40	176.52	19.17
50 Hz	1100	8.1	67.63	7.21	73.58	324.06	43.33
	600	4.6	70.41	6.68	75.93	179.63	18.88
Constant Field	1100	8.0	66.80	7.23	72.77	321.20	43.15
	600	4.5	68.88	6.64	74.36	176.29	18.65
Distilled water	1100	5.6	46.77	6.89	52.46	242.90	33.44
	600	3.1	47.47	6.44	52.79	131.51	14.60
PV with no collector	1100	–	–	5.32	4.39	52.44	19.93
	600	–	–	5.37	4.43	28.85	10.96

Table 4
3 wt% Fe_3O_4 and distilled water.

	Radiation (W/m²)	$\Delta T_{collector}$ (°C)	η_{th} (%)	η_{el} (%)	η_{pvt} (%)	Overall thermal output (W)	Overall exergy output (W)
No field	1100	8.2	68.42	7.23	74.39	327.25	45.23
	600	4.7	71.90	6.71	77.44	182.83	19.51
5 Hz	1100	8.3	69.26	7.18	75.19	329.93	45.66
	600	4.8	73.43	6.74	79.00	186.08	19.54
25 Hz	1100	8.6	71.76	7.18	77.69	339.30	47.25
	600	4.8	73.43	6.78	79.03	186.31	20.00
50 Hz	1100	8.7	72.59	7.28	78.60	343.36	48.08
	600	4.9	74.96	6.81	80.58	189.62	20.39
Constant Field	1100	8.1	67.59	7.18	73.52	323.60	45.32
	600	4.6	70.37	6.77	75.96	180.00	18.88
Distilled water	1100	5.6	46.77	6.89	52.46	242.90	33.44
	600	3.1	47.47	6.44	52.79	131.51	14.60
PV with no collector	1100	–	–	5.32	4.39	52.44	19.93
	600	–	–	5.37	4.43	28.85	10.96

Table 5
Fractional uncertainties.

$\delta\eta_{th}/\eta_{th}$	$\delta\eta_{el}/\eta_{el}$	$\delta\dot{E}x_{th}/\dot{E}x_{th}$
±0.0094	±0.012	±0.0165
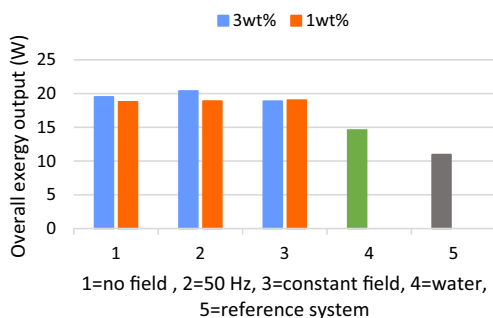
Fig. 14. Overall exergy output for 1 wt% and 3 wt% ferrofluid under magnetic field (300G) and 600 W/m² radiation.

again indicates that using a constant magnetic field is not preferred over the ferrofluid with no field at all. For Case 4 with an alternating magnetic field, however, the overall thermal output for 3 wt% ferrofluid reaches a value of 343.36 W which shows nearly 5% improvement compared to Case 2 with no magnetic field.

The overall thermal output for 600 W/m² solar radiation is shown in Fig. 12. It is clear from the figure that the use of ferrofluid improved the system overall thermal output compared to that of Case 1 (collector with distilled water) and Case 5 (system without collector). The overall thermal output is 28.85 W for Case 5, and 131.51 W, 176.52 W and 182.83 W for Case 1, and Case 2 with 1 wt% and 3 wt% ferrofluid, respectively.

Fig. 13 illustrates the system overall exergy for 1100 W/m² solar radiation. As seen from the figure for the case without applying any field (Case 2) the exergy output is 42.81 W and 45.23 W for 1 wt% and 3 wt% ferrofluid, respectively, whereas this amount for Case 1 is 33.44 W and for Case 5 is 19.93 W. Therefore, it is observed that using ferrofluid results in a maximum of 39% improvement in comparison to distilled water (Case 1). The exergy output for Case 3 for both concentrations are close to that of Case 2. For Case 4 with an alternating magnetic field, about 6% increase is seen for the exergy output in comparison to Case 2 for 3 wt% ferrofluid.

Fig. 14 shows the variations of overall exergy output for 600 W/m² solar radiation. In this radiation, a maximum exergy output of about 20.39 W is observed which again related to Case 4 with 3 wt% ferrofluid. The exergy output for distilled water is nearly 14.6 W.

For a better comparison between various cases explained, the entire collected experimental data are given in Table 3 and Table 4 for 1 wt% and 3 wt% ferrofluid, respectively. In order to compare different cases of ferrofluid to the PVT system with distilled water and the reference system (PV with no collector), the corresponding amounts for these two systems are repeated in both Tables. As seen from Table 3, the maximum overall efficiency of the system calculated from Eq. (5) is 71.91% and 74.4% for 1 wt% ferrofluid for 1100 W/m² and 600 W/m² solar radiation, respectively. It is also observed a nearly 40% improvement in overall efficiency for Case 4 in comparison with that of Case 1. In Table 3 it is also shown that increasing the frequency of alternating magnetic field from 5 Hz to 50 Hz results in negligible variation in thermal and overall efficiencies of the system. For 3 wt% ferrofluid

(Table 4), however, a small increase in efficiencies are observed when the frequency of the magnetic field increases from 5 to 50 Hz.

6. Conclusion

The effects of a ferrofluid on the efficiency of a PVT system (consisting of a combined PV module and an absorber collector) under two solar radiations were investigated. The performances of four different cases including the collector with distilled water, ferrofluid with no magnetic field, ferrofluid with a constant magnetic field, and ferrofluid with an alternating magnetic field of 50 Hz for two concentrations (1 wt% and 3 wt%) were compared to that of the PV module with no collector. Two solar radiations of 1100 W/m^2 and 600 W/m^2 were tested in the experiments by using a solar simulator designed to perform in indoor conditions. The major findings of the experiments can be summarized as:

- The overall efficiency of the system reached to about 52% when distilled water was used as the cooling fluid in the collector. This value can be compared to that of the PV module with no collector which was only 4.4%.
- Changing the cooling fluid from distilled water to a ferrofluid, i.e. Fe_3O_4-water, the overall efficiency of the system for 3 wt% concentration improved by about 76%.
- The effect of an alternating magnetic field with 50 Hz frequency for 3 wt% ferrofluid was about 4–5% in the overall efficiency compared to the value obtained for the same conditions with no magnetic field.
- The thermal efficiency of ferrofluid for a constant magnetic field was very close to that of the system when no field was applied.
- The overall exergy of the system in the case of an alternating magnetic field with 50 Hz frequency reached as high as 48 W. This amount for the case of distilled water was only about 33 W.

The experiments performed in the course of this study reveal that adding a thermal collector to a PV module and using a 3 wt% ferrofluid accompanied by an alternating magnetic field with 50 Hz frequency can improve the overall efficiency of the system to about 79%.

Acknowledgements

References

[1] Chow TT. A review on photovoltaic/thermal hybrid solar technology. Appl Energy 2010;87:365–79.
[2] Kalogirou SA, Tripanagnostopoulos Y. Hybrid PV/T solar systems for domestic hot water and electricity production. Energy Convers Manage 2006;47: 3368–82.
[3] Prakash J. Transient analysis of a photovoltaic-thermal solar collector for co-generation of electricity and hot air/water. Energy Convers Manage 1994;35: 967–72.
[4] Sopian K, Yigit KS, Liu HT, Kakac S, Veziroglu TN. Performance analysis of photovoltaic thermal air heaters. Energy Convers Manage 1996;37: 1657–70.
[5] Sopian K, Liu HT, Kakac S, Veziroglu TN. Performance of a double pass photovoltaic thermal solar collector suitable for solar drying systems. Energy Convers Manage 2000;41:353–65.
[6] Hegazy AA. Comparative study of the performances of four photovoltaic/ thermal solar air collectors. Energy Convers Manage 2000;41:861–81.
[7] Chow TT, Pei G, Fong KF, Lin Z, Chan ALS, Ji J. Energy and exergy analysis of photovoltaic thermal collector with and without glass cover. Appl Energy 2009;86:310–6.
[8] Gang P, Hide F, Tao Z, Jie J. A numerical and experimental study on a heat pipe PV/T system. Sol Energy 2011;85:911–21.
[9] Dubey S, Sandha GS, Tiwari GN. Analytical expression for efficiency of PV/T hybrid air collector. Appl Energy 2009;86:697–705.
[10] Bahaidarah H, Subhan A, Gandhidasan P, Rehman S. Performance evaluation of a PV (photovoltaic) module by back surface water cooling for hot climatic conditions. Energy 2013;59:445–53.
[11] Daghigh R, Ruslan MH, Sopian K. Advances in liquid based photovoltaic/ thermal (PV/T) collectors. Renew Sustain Energy Rev 2011;15:4156–70.
[12] Yun CUI, Qunzhi ZHU. Study of photovoltaic/thermal systems with MgO/water nanofluids flowing over silicon solar cells. Power and energy engineering conference (APPEEC). 2012.
[13] Yousefi T, Veysi F, Shojaeizadeh E, Zinadini S. An experimental investigation on the effects of Al_2O_3.H_2O nanofluid on the efficiency of flat-plate solar collectors. Renewable Energy 2012;39:293–8.
[14] Sardarabadi M, Passandideh-Fard M, Zeinali HS. Experimental investigation of the effects of silica/water nanofluid on PV/T (photovoltaic thermal units). Energy 2014;66:264–72.
[15] Li Q, Xuan Y. Experimental investigation on heat transfer characteristics of magnetic fluid flow around a fine wire under the influence of an external magnetic field. Exp Thermal Fluid Sci 2009;33:591–6.
[16] Lajvardi M, Moghimi-Rad J, Hadi I, Gavili A, Dallali Isfahani T, Zabihi F, et al. Experimental investigation for enhanced ferrofluid heat transfer under magnetic field effect. J Magn Magn Mater 2010;322:3508–13.
[17] Ghofrani A, Dibaei MH, Hakim Sima A, Shafii MB. Experimental investigation on laminar forced convection heat transfer of ferrofluids under an alternating magnetic field. Exp Thermal Fluid Sci 2013;49:193–200.
[18] Azizian R, Doroodchi E, McKrell T, Buongiorno J, Hu LW, Moghtaderi B. Effect of magnetic field on laminar convective heat transfer of magnetite nanofluids. Int J Heat Mass Transf 2014;68:94–109.
[19] Ibrahim A, Othman MY, Ruslan MH, Mat S, Sopian K. Recent advances in flat plate photovoltaic/thermal (PV/T) solar collectors. Renew Sustain Energy Rev 2011;15:352–65.
[20] Nkurikiyimfura I, Wanga Y, Pan Z. Heat transfer enhancement by magnetic nanofluids—a review. Renew Sustain Energy Rev 2013;21:548–61.
[21] Haddad Z, Abid C, Oztop HF, Mataoui A. A review on how the researchers prepare their nanofluids. Int J Therm Sci 2014;76:168–89.
[22] Es'haghi Z, Heidari T, Mazloomi E. In situ pre-concentration and voltammetric determination of trace lead and cadmium by a novel ionic liquid mediated hollow fiber-graphite electrode and design of experiments via Taguchi method. Electrochim Acta 2014;147:279–87.
[23] Lopez JA, González F, Bonilla FA, Zambrano G, Gómez ME. Synthesis and characterization of Fe_3O_4 magnetic nanofluid. Revista Latinoamericana de Metalurgia y Materiales 2010;30:60–6.
[24] Drew DA, Passman SL. Theory of multicomponent fluids. 1st ed. Germany: Springer; 1999.
[25] Chow TT, He W, Ji J. Hybrid photovoltaic-thermosyphon water heating system for residential application. Sol Energy 2006;80:298–306.
[26] Agrawal S, Tiwari GN. Energy and exergy analysis of hybrid micro-channel photovoltaic thermal module. Sol Energy 2011;85:356–70.
[27] Garg HP, Agarwal RK. Some aspects of a PV/T collector forced circulation flat plate solar water heater with solar cells. Energy Convers Manage 1995;36: 87–99.
[28] Chenming H, White RM. Solar cells from basic to advanced systems. New York: McGraw-Hill; 1983.
[29] Kumar R, Rosen MA. Performance evaluation of a double pass PV/T solar air heater with and without fins. Appl Therm Eng 2011;31:1402–10.
[30] Tiwari A, Dubey S, Sandhu GS, Sodha MS, Anwar SI. Exergy analysis of integrated photovoltaic thermal solar water heater under constant flow rate and constant collection temperature modes. Appl Energy 2009;86:2592–7.
[31] Fudholi A, Sopian K, Yazdi MH, Ruslan MH, Ibrahim A, Kazem HA. Performance analysis of photovoltaic thermal (PVT) water collectors. Energy Convers Manage 2014;78:641–51.
[32] Taylor JR. An introduction to error analysis: the study of uncertainties in physical measurements. Sausalito: University Science Books; 1997.
[33] Huang BJ, Lin TH, Hung WC, Sun FS. Performance evaluation of solar photovoltaic/thermal systems. Sol Energy 2001;70:443–8.